

## DEVELOPMENT OF A NOVEL SYNTHESIS METHOD OF A RIGID-BODY FOUR-BAR LINKAGE INTO A COMPLIANT MECHANISM

*Estefania Hermoza-Llanos<sup>1</sup>, Jorge A. Rodríguez-Hernández<sup>2</sup> and Lena Zentner<sup>3</sup>*

<sup>1</sup> Mechanical Engineering, Institute of Mechanism Theory, Machine Dynamic and Robotics, RWTH Aachen University, Eilfschornsteinstraße 18, 52062 Aachen, Germany.

<sup>2</sup> Mechanical Engineering, Academic Department of Engineering - Mechanical Engineering Section, Pontificia Universidad Católica del Perú, Av. Universitaria N° 1801, San Miguel 15088, Lima, Perú.

<sup>3</sup> Mechanical Engineering, Compliant Systems Group, Technische Universität Ilmenau, Max-Planck-Ring 12, Werner-Bischoff-Bau, WB 2260, 98684 Ilmenau, Germany.

### ABSTRACT

The four-bar linkage mechanism is widely used in various machinery applications. This study presents a synthesis method to transform a rigid-body four-bar mechanism into a compliant mechanism using four leaf-type hinges based on linear theory and Castigliano's Theorem. The objective is to determine the dimensions and configuration of a flexible four-bar mechanism that replicates the behavior of the initial rigid-body mechanism. The meeting point between the two mechanisms is the flexure hinge of the compliant mechanism, which is determined using the Pseudo-Rigid-Body model (PRBM). To validate the proposed method, a program based on non-linear theory is employed. The results confirm that the dimensional differences between the two are minimal, ranging from 0% to 0.13%. This study demonstrates the feasibility of synthesizing a Rigid-Body Four-Bar Mechanism into a compliant mechanism using the PRBM, as long as the deformations are within the linear domain.

**Index Terms** – Compliant mechanism, four-bar mechanism, Pseudo-Rigid-Body model, linear domain.

### 1. INTRODUCTION

A new breed of mechanisms has emerged that challenges the reliance on rigid parts: compliant mechanisms. Unlike their rigid counterparts, compliant mechanisms achieve the conversion and transmission of movements and forces through the deflection or elastic deformation of their flexible components, without the need for hinges or sliding joints. Remarkably, compliant mechanisms can be found in nature, such as the intricate opening and closing systems of flowers, the wings of mosquitoes, elephant trunks, seaweed, and eels [1].

Compliant mechanisms offer numerous advantages over rigid-body mechanisms, as extensively detailed in the Handbook of Compliant Mechanisms by Larry Howell [1]. These advantages include the ability to be manufactured as a single piece, reducing assembly time, simplifying manufacturing processes, and enabling seamless integration of form and function. Moreover, compliant mechanisms tend to be lighter compared to their rigid counterparts, necessitate less



lubrication, minimize noise and vibrations, and offer enhanced mechanical precision due to fewer joints. Additionally, the deflection of their flexible members allows for the storage and release of strain energy, making them invaluable in applications where space-saving is crucial, such as MEMS devices.

Among the diverse array of rigid-body mechanisms, the four-bar linkage holds particular importance. It plays a pivotal role in numerous everyday devices, including bicycle suspensions, pumpjacks, sewing machines, oscillating fans, and windshield wipers. The four-bar linkage consists of four bars interconnected by four joints, with the configuration and movement dependent on the lengths of the links, as defined by Grashof's law. While traditionally limited to rigid body mechanisms, compliant configurations of the four-bar linkage have gained prominence in recent times. Although these compliant versions allow only small displacements, they have extensive applications, particularly in the field of precision engineering.

The advent of compliant mechanisms has revolutionized the field of mechanical systems, offering a viable alternative to conventional rigid-body mechanisms. Their flexible nature, coupled with numerous advantages such as reduced energy loss, lightweight design, decreased need for lubrication, and improved precision, has paved the way for their extensive use in various industries and applications. Furthermore, the four-bar linkage stands out as a crucial mechanism, now also applicable in compliant configurations, while hybrid models combine the strengths of compliant and rigid components. The following sections of this paper will delve deeper into the feasibility of synthesizing a Rigid-Body Four-Bar Mechanism into a compliant mechanism using the Pseudo-Rigid-Body model (PRBM), as long as the deformations are within the linear domain.

The rest of the paper is organized as follows. Section 2 presents the state of the art of the research. Section 3 describes the methodology followed and a description of the algorithm's development. Two synthesized mechanisms were compared with a program based on the non-linear theory in order to present them as a design verification in Section 4 and finally, conclusions and some future work are drawn in Section 5.

## 2. RELATED WORK

This section presents the replacement of rigid-body mechanisms with compliant mechanisms and the iterative process of synthesis and analysis through previous researches. The forces in the system must be considered to calculate the appropriate compliant hinge.

To achieve accurate results, idealized rigid-body models and PRBM based on different joint discretization methods are used for analysis and modeling. An iterative process is required to find an appropriate solution. Each type of rigid-body mechanism has different characteristics, making the synthesis non-generalizable. In this work, the focus is on the synthesis of a four-bar compliant mechanism.

Saggere, *et al.* [2] present a technique that treats the three links of the four-bar mechanism as a slender flexible segment. It uses the slope-deflection equation of the moment distribution method to calculate moments, forces, and deflections. Non-linear deflections of the beams are considered, and a finite-link model with torsional springs is used for numerical analysis. Howell, *et al.* [1] present in the book named "Handbook of Compliant Mechanisms" the PRBM for synthesizing compliant mechanisms. The PRBM integrates the movement and forces of a

compliant mechanism by modeling it as a rigid-body mechanism. The synthesis process involves identifying the rigid-body model, replacing rigid links and/or movable joints with compliant members, developing the pseudo-rigid-body model, and selecting materials and sizing the compliant members. Valentini, *et al.* [3] used a methodology that involves modeling the four flexure hinges using a planetary arrangement, capturing the relative motion between connected parts. This methodology is based on the use of second-order pseudo-rigid complexes able to accurately approximate the deformation of flexure hinges undergoing large displacements.

### 3. METHODOLOGY

This synthesis method pretends to synthesize a Rigid-Body Four-Bar mechanism into its compliant version using PRBM and staying in the linear domain. Figure 1 illustrates in blue lines the initial configuration of the four-bar linkage and its synthesized compliant mechanism with all the measurements needed.

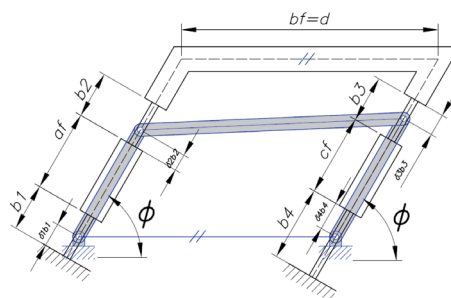


Figure 1 – Initial configuration. In grey Four-Bar linkage rigid mechanism. In white Compliant Four-Bar linkage synthesized.

The compliant mechanism was shown in a deflected position due to an applied force, which could be positioned either at the top or on one side. These configurations shared the same angle  $\phi$  and a constant dimension  $d$  at the base of the compliant mechanism.

#### 3.1 Pseudo-Rigid-Body Model

The deflection of compliant hinges is caused by internal forces or moments resulting from external forces. The pseudo-rigid-body model is used to understand this behavior, which describes a correspondence between the motion and force of an elastic member and a rigid-body mechanism, as seen in Figure 2. The compliant bar is replaced with a rigid-body system where flexibility is simulated by a torsion spring, providing torsional stiffness and determining the spring's position. Assumptions made for this model include linearity, small deformations, and a constant cross section for the compliant system. In the linear theory, the displacement of the flexure hinge must be less than 10% of its total length.

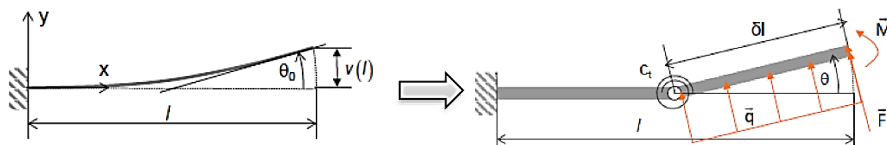


Figure 2 – Modeling of a compliant system as a rigid-body system [4]

A set of equations representing the model of a compliant system as a rigid-body system is derived using the symbology shown in Figure 2. The model assumes the presence of one force and one moment at the end of the bar, resulting in Equation (1) as described.

$$\delta = \frac{3M + 2FL}{6M + 3FL} \quad (1)$$

Where:

- M: Internal moment at the end of the compliant hinge.
- F: Internal shear force at the end of the compliant hinge.
- L: Length of the compliant hinge.

### 3.2 Study cases

We have two distinct study cases available. In the first case, the force is applied at one side of the structure, while in the second case, the force is applied at the top. The bases of the structures may not be at the same level. Figure 3 illustrates the division of the structures into sections  $x1$ ,  $x2$ ,  $x3$ , and  $x4$ . This division allows us to apply the Castigliano's theorem, enabling different analyses for each section.

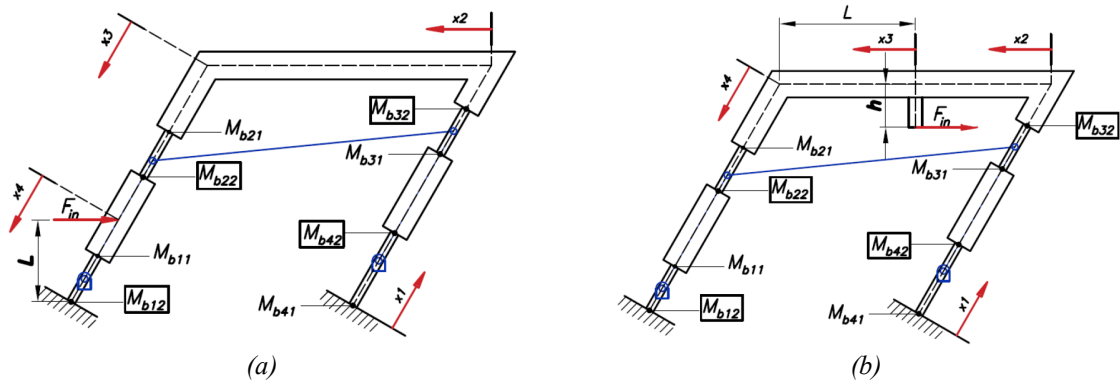


Figure 3 – Study cases. (a) Force at one side. (b) Force at the top.

To begin the analysis, we need to examine the external forces for each case by utilizing a free body diagram, as depicted in Figure 4. It is important to note that each study case presents two additional subdivisions for each case, namely when the right side is longer or when the left side is longer. In this paper, we will focus on presenting the analysis for one specific type: the force applied at the top with the right side longer. The other three cases undergo the same analysis, and the complete equations can be found in the Master thesis *Development of methods for the synthesis of compliant mechanisms* [5].

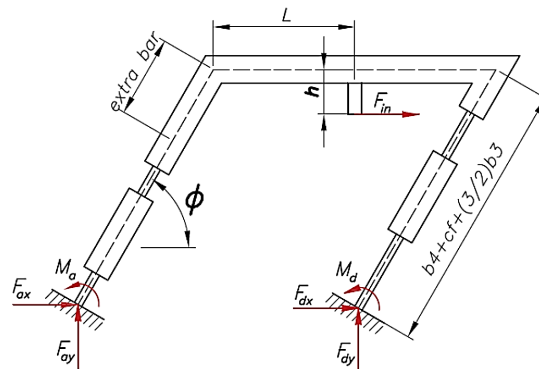


Figure 4 – Free body diagram for the case “Applied force at the top and right side longer”.

The following equations result from the sum of forces:

$$F_{dx} = -F_{ay} \quad (2)$$

$$F_{dx} = -F_{in} - F_{ax} \quad (3)$$

$$M_d = -M_a - F_{ax}L_1 + F_{ay}L_2 + F_{in}L_3 \quad (4)$$

Where:

$$L_1 = \sin\phi(\delta_1b_1 - b_4 + \delta_4b_4)$$

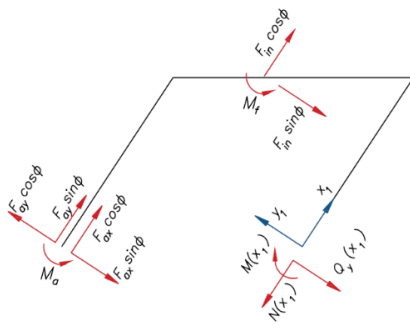
$$L_2 = d + \cos\phi(\delta_1b_1 - b_4 + \delta_4b_4)$$

$$L_3 = \sin\phi\left(b_4 + cf + \frac{3}{2}b_3\right) - h$$

The next step is to divide the structure into four sections to apply Castigliano's theorem in a next step. Based on the sections represented in Figure 3.b., the analysis of internal forces are presented for the case "Applied force at the top and right side longer".

### Section 1:

$$0 < x_1 < b_4 + cf + \frac{3}{2}b_3$$



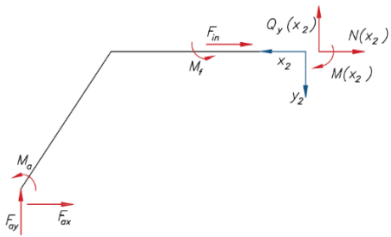
$$N(x_1) = F_{in} \cos \phi + F_{ax} \cos \phi + F_{ay} \sin \phi \quad (5)$$

$$Q_y(x_1) = -F_{in} \sin \phi - F_{ax} \sin \phi + F_{ay} \cos \phi \quad (6)$$

$$M(x_1) = -F_{in} \left[ \left( b_4 + cf + \frac{3}{2}b_3 - x_1 \right) \sin \phi \right] + F_{ax} [(x_1 - b_4 + b_4\delta_4 + b_1\delta_1) \sin \phi] - F_{ay} [(x_1 - b_4 + b_4\delta_4 + b_1\delta_1) \cos \phi + d] + M_a + M_f \quad (7)$$

### Section 2:

$$0 < x_2 < d - L$$



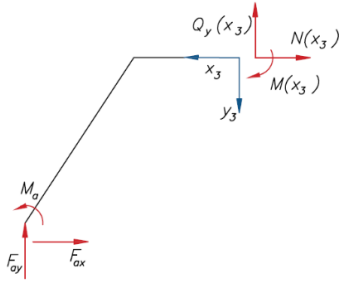
$$N(x_2) = -F_{in} - F_{ax} \quad (8)$$

$$Q_y(x_2) = -F_{ay} \quad (9)$$

$$M(x_2) = F_{ax} \left( c + \delta_1b_1 + \delta_3b_3 + \frac{1}{2}b_3 \right) \sin \phi - F_{ay} \left[ \left( c + \delta_1b_1 + \delta_3b_3 + \frac{1}{2}b_3 \right) \cos \phi + d - x_2 \right] + M_a + M_f \quad (10)$$

### Section 3:

$$d - L < x_3 < d$$



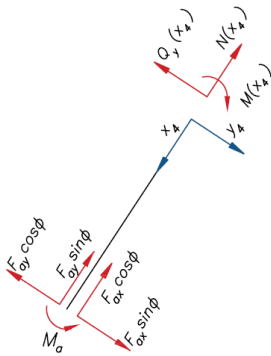
$$N(x_3) = -F_{ax} \quad (11)$$

$$Q_y(x_3) = -F_{ay} \quad (12)$$

$$M(x_3) = F_{ax} \left( c + \delta_1 b_1 + \delta_3 b_3 + \frac{1}{2} b_3 \right) \sin \phi - F_{ay} \left[ \left( c + \delta_1 b_1 + \delta_3 b_3 + \frac{1}{2} b_3 \right) \cos \phi + d - x_3 \right] + M_a \quad (13)$$

### Section 4:

$$0 < x_4 < b_4 + cf + \frac{3}{2} b_3$$



$$N(x_4) = -F_{ax} \cos \phi - F_{ay} \sin \phi \quad (14)$$

$$Q_y(x_4) = F_{ax} \sin \phi - F_{ay} \cos \phi \quad (15)$$

$$M(x_4) = F_{ax} \sin \phi \left( c + \delta_1 b_1 + \delta_3 b_3 + \frac{1}{2} b_3 - x_4 \right) - F_{ay} \cos \phi \left( c + \delta_1 b_1 + \delta_3 b_3 + \frac{1}{2} b_3 - x_4 \right) + M_a \quad (16)$$

### 3.3 Castigliano's Theorem

The Castigliano's theorem states that the first partial derivative of the total internal energy in a structure with respect to a force applied at any point is equal to the deflection at that point in the direction of the force's line of action. This theorem can be used to determine equilibrium forces in the hyperstatic structures of this research.

The study cases represented in Figure 3 require three equations to determine six external forces. To achieve this, the Castigliano's theorem is applied, providing six equations for the six variables. To obtain the additional three equations needed, the forces  $F_{ay}$ ,  $F_{ax}$ , and  $M_a$  are considered. These forces do not cause deflection or rotation. The equations for each of these forces are provided in equations (17), (18) and (19).

- $F_{ay} \rightarrow$  No deflection

$$0 = \int_S \frac{N(x)}{E \cdot A} \cdot \frac{\partial N(x)}{\partial F_{ay}} dx + \int_S \frac{Q_y(x)}{Q \cdot \kappa \cdot A} \cdot \frac{\partial Q_y(x)}{\partial F_{ay}} dx + \int_S \frac{M_z(x)}{E \cdot I_z} \cdot \frac{\partial M_z(x)}{\partial F_{ay}} dx \quad (17)$$

- $F_{ax} \rightarrow$  No deflection

$$0 = \int_S \frac{N(x)}{E \cdot A} \cdot \frac{\partial N(x)}{\partial F_{ax}} dx + \int_S \frac{Q_y(x)}{Q \cdot \kappa \cdot A} \cdot \frac{\partial Q_y(x)}{\partial F_{ax}} dx + \int_S \frac{M_z(x)}{E \cdot I_z} \cdot \frac{\partial M_z(x)}{\partial F_{ax}} dx \quad (18)$$

- $M_a \rightarrow$  No rotation

$$0 = \int_S \frac{N(x)}{E \cdot A} \cdot \frac{\partial N(x)}{\partial M_a} dx + \int_S \frac{Q_y(x)}{Q \cdot \kappa \cdot A} \cdot \frac{\partial Q_y(x)}{\partial M_a} dx + \int_S \frac{M_z(x)}{E \cdot I_z} \cdot \frac{\partial M_z(x)}{\partial M_a} dx \quad (19)$$

Each equation must be applied to each case in order to express  $F_{ay}$ ,  $F_{ax}$ , and  $M_a$  in terms of  $b_1$ ,  $b_2$ ,  $b_3$ ,  $b_4$ ,  $a_f$ , and  $c_f$ . Each section may have different areas and inertias, so the integral is divided accordingly. The developed equations can be found in the Master thesis *Development of methods for the synthesis of compliant mechanisms* [5]

### 3.4 Final equations

After formulating the equations for external forces and internal forces using Castigliano's theorem, we can proceed to apply the PRBM to determine the location of the equivalent torsional spring. Additionally, the equations for the maximum stress and the corresponding geometry can be found, which establish the equivalence between the rigid-body mechanism and the compliant one. The subsequent text provides these equations for the reader's reference.

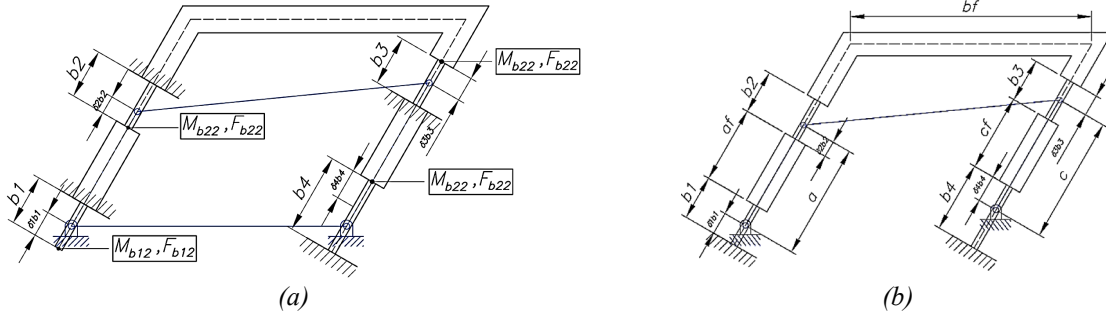


Figure 5 – Diagrams for final equations. (a) Internal forces and moments configuration. (b) Diagram of geometry connections between the compliant and the rigid-body mechanisms.

#### 3.4.1 PRBM equations

The equivalence between the rigid-body mechanism and the synthesized compliant mechanism is defined by the position of the torsional spring equivalent, which must be placed at the same point as the joint of the rigid-body mechanism.

As seen in Section 3.1, the symbol  $\delta$  represents the portion of the bar where this torsional spring is located.

$$\delta_1 = \frac{1}{3} \frac{3M_{b12} + 2F_{b12}b_1}{2M_{b12} + F_{b12}b_1} \quad (20)$$

$$\delta_2 = \frac{1}{3} \frac{3M_{b22} + 2F_{b22}b_2}{2M_{b22} + F_{b22}b_2} \quad (21)$$

$$\delta_3 = \frac{1}{3} \frac{3M_{b32} + 2F_{b32}b_3}{2M_{b32} + F_{b32}b_3} \quad (22)$$

$$\delta_4 = \frac{1}{3} \frac{3M_{b42} + 2F_{b42}b_4}{2M_{b42} + F_{b42}b_4} \quad (23)$$

Where:

- $\delta_i$  : Portion of the bar where is ubicated the torsion spring equivalent.

- $M_{bi2}$  : The moment at the end of the bar.
- $F_{bi2}$  : The shear force at the end of the bar.
- $b_i$  : The length of the compliant hinge.

### 3.4.2 Required maximum stress equations

Furthermore, the material properties were taken into account, assuming that each joint operates at a maximum specified stress level with a safety factor incorporated.

$$\frac{\sigma_y}{SF} = \sigma_{eq_{b1}} = \sqrt{\sigma_{b1}^2 + 3\tau_{b1}^2} \quad (24)$$

$$\frac{\sigma_y}{SF} = \sigma_{eq_{b2}} = \sqrt{\sigma_{b2}^2 + 3\tau_{b2}^2} \quad (25)$$

$$\frac{\sigma_y}{SF} = \sigma_{eq_{b3}} = \sqrt{\sigma_{b3}^2 + 3\tau_{b3}^2} \quad (26)$$

$$\frac{\sigma_y}{SF} = \sigma_{eq_{b4}} = \sqrt{\sigma_{b4}^2 + 3\tau_{b4}^2} \quad (27)$$

Where:

- $\sigma_y$  : Yield strength of the material.
- $SF$  : Safety factor.
- $\sigma_{eq_{bi}}$  : Equivalent tensile stress (Von Mises yield criterion).
- $\sigma_{bi}$  : Bending stress.
- $\tau_{bi}$  : Torsional stress.

### 3.4.3 Geometry equations

The final equations establish the relationships between the geometry of the compliant system and the corresponding rigid-body system. These equations are visually represented in the following figure.

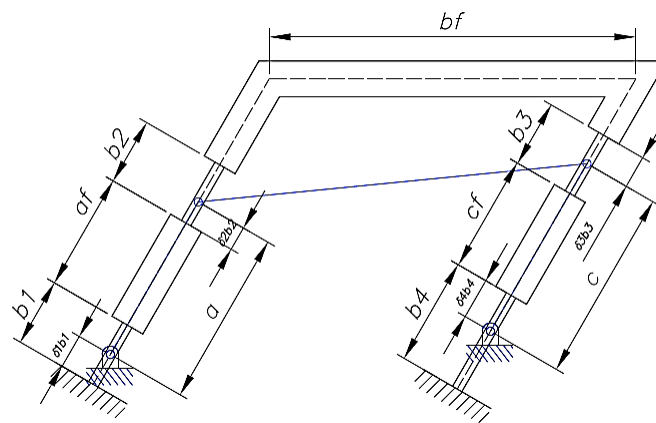


Figure 6 – Geometry of the structure

$$b_1 - \delta_1 b_1 + af + \delta_2 b_2 = a \quad (28)$$

$$b_3 - \delta_3 b_3 + cf + \delta_4 b_4 = c \quad (29)$$



Where:

- $b_i$  : The length of the compliant hinge.
- $\delta_i$  : Portion of the bar where is ublicated the torsion spring equivalent.
- $cf$  : Right bar of the compliant mechanism.
- $af$  : Left bar of the compliant mechanism.
- $a$  : Right bar of the rigid-body system.
- $b$  : Left bar of the rigid-body system.

With this set of equations  $b_1, b_2, b_3, b_4, \delta_1, \delta_2, \delta_3, \delta_4, af$  and  $cf$  can be calculated implementing an algorithm in MATLAB, which depends on the specific case of analysis. By finding all the aforementioned variables, the forces  $F_{ax}, F_{ay}$ , and the moment  $M_a$  can be known through the application of Castigliano's theorem. Consequently, all the equations can be solved.

With the obtained values, the configuration of the compliant mechanism is defined, along with the internal forces present in each considered section.

#### 4. DESIGN VERIFICATION AND RESULTS

The research's effectiveness is verified through a comparison with another program based on non-linear theory. *Numerical calculation approach based on non-linear theory for large deflections of curved rod-like structures* is a research that contains a software in MATLAB with a non-linear numerical calculation to evaluate output parameters such as straight-line deviation, coupler rotation, elastic strain distribution, maximum strain, and displacement for different versions of the parallel four-bar linkage with curved coupler hinges or curved coupler links [6].

The comparison between the two programs begins with selecting an example obtained from the algorithm presented in the analytical design. The results from this algorithm are considered as input data for the non-linear theory program.

The deltas of the flexure hinges ( $\delta_1, \delta_2, \delta_3$  and  $\delta_4$ ) are the crucial values for comparison. While the algorithm calculates these values, the non-linear theory program requires obtaining the delta values through the angles of deflection. The non-linear theory program involves numerous parameters, including the lengths of the compliant mechanism's configuration, force, and material characteristics, which are determined by the results of the synthesis algorithm. These parameters can be seen in the Figure 7.

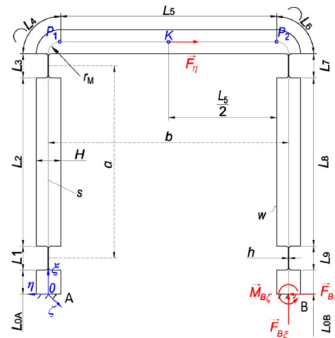


Figure 7 – Geometric input parameters for a compliant parallel mechanism.

Once the synthesis algorithm determines the configuration of the compliant mechanism equivalent to the rigid-body system, these measurements are incorporated into the non-linear theory program to compare the positions based on delta values in each compliant hinge and obtain the values of the links in the rigid-body system. Two synthesized mechanisms were considered as input data for the non-linear theory program; its configuration and dimensions can be seen in the Figure 8 and Table 1.

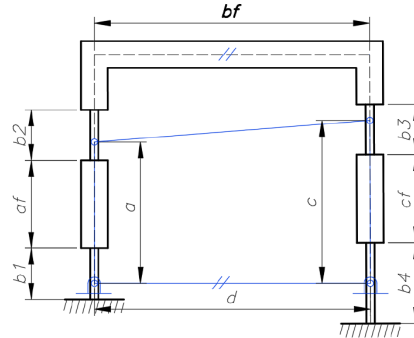


Figure 8 – Schematic compliant four-bar mechanism synthesized. In blue, the rigid-body mechanism; in black, the equivalent compliant mechanism.

Table 1 – Geometric resulting values

	$b_1$ [mm]	$b_2$ [mm]	$b_3$ [mm]	$b_4$ [mm]	$cf$ [mm]	$af$ [mm]	Time of simulation
<b>Synthesized Mechanism 1</b>	18.89	12.56	54.40	15.37	24.85	83.33	10.65 min
<b>Synthesized Mechanism 2</b>	8.90	5.91	27.38	7.20	9.90	42.18	8.58 min

The inputs seen in the Table 1 were used in the non-linear program and the results (position of the flexure hinges) were compared with the initial configuration of the rigid body four-bar linkage of the synthesized mechanisms. The comparison can be seen in Figure 9 and Table 2. A slight difference between the two analyses (less than 0.5%) appears and is considered accurate for small deformations due to applied loads. The length "d" shows no difference as it was taken as an input in the non-linear analysis. The deformed shape of the compliant mechanism is shown, indicating that each flexure hinge operates within the linear field due to small displacements.

Table 2 – Results and verification.

		$a$ [mm]	$b$ [mm]	$c$ [mm]	$d$ [mm]
<b>Example 1</b>	Inputs – Linear theory	100	63.246	80	60
	Nonlinear theory	100.02	63.196	79.928	60
	<b>Difference</b>	<b>-0.02%</b>	<b>0.08%</b>	<b>0.09%</b>	<b>0.00%</b>
<b>Example 2</b>	Inputs – Linear theory	50	60.828	40	60
	Nonlinear theory	50.003	60.817	39.948	60
	<b>Difference</b>	<b>-0.01%</b>	<b>0.02%</b>	<b>0.13%</b>	<b>0.00%</b>

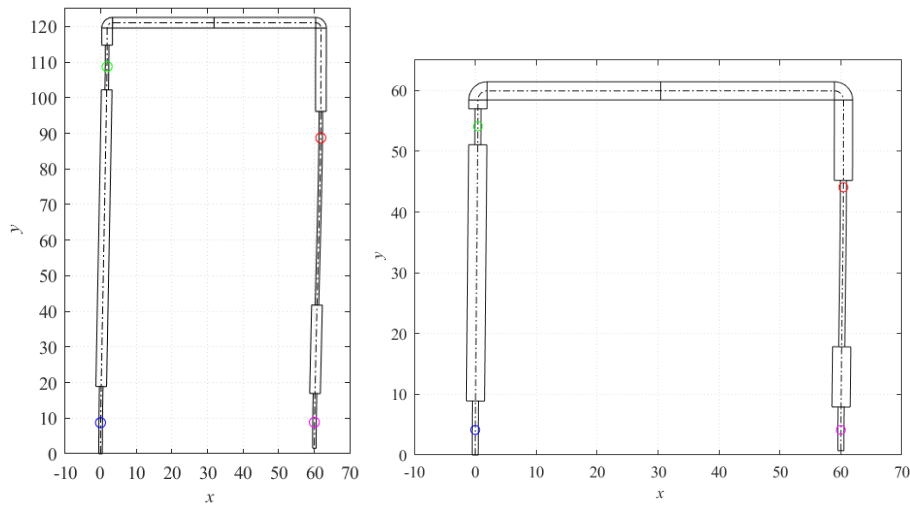


Figure 9 – Results of the numerical calculation based on the non-linear theory.

## 5. CONCLUSIONS

The synthesis of rigid body systems into compliant mechanisms is a complex task that varies according to the specific mechanism type. In this study, we focused on the four-bar link mechanism and successfully applied Castigliano's theorem to analyze the moments and internal forces. Dividing the system into sections based on the applied force and considering changes in the reference system and cross-sectional area were critical for effectively applying Castigliano's theorem. The numerical tools used in this study, provided precise results for determining the external forces. Additionally, the Levenberg-Marquardt and trust-region methods were employed to determine the configuration of the compliant mechanism. It was essential to establish reliable initial values to ensure accurate results and mitigate unwanted outcomes, given the sensitivity of the "fsolve" function in Matlab. Working within the linear field was highly important, as it guaranteed that the working force generated only small displacements in each flexure hinge. Furthermore, achieving high precision in the manufacturing process of the compliant mechanism is crucial to realize the calculated high accuracy.

Future analysis could focus on demonstrating the displacement of the resulting compliant mechanism under different applied forces. This would provide a more comprehensive understanding of the system's behavior and validate the effectiveness of the design approach. The computational time required to obtain solutions can be lengthy. To address this, it is important to improve the determination of initial values or explore alternative numerical tools capable of efficiently solving the nonlinear polynomial system of equations. This would significantly reduce the overall calculation time and enhance the practical applicability of the design methodology. Incorporating dimensionless data in the analysis can contribute to establishing reliable initial values for various cases. By normalizing the data, the system's behavior could be better understood, and initial guesses can be made with greater confidence. Exploring the effects of changing the force direction and introducing an angle to the force can open up new design possibilities for compliant mechanisms. This would require the calculation of new systems of equations for each section, considering different types of flexure hinges. Possible options include corner-filletted contour with varying radius, elliptical contour, and variable power function-based contour.

In conclusion, this study has provided valuable insights into the synthesis of compliant mechanisms, particularly focusing on the four-bar link mechanism. The successful application

of Castigliano's theorem and the utilization of numerical tools have paved the way for future advancements. By addressing the outlined future directions and implementing suggested improvements, researchers can further enhance the design and analysis of compliant mechanisms in various applications.

## REFERENCES

- [1] L. Howell, S. Magleby and B. Olsen, Handbook of Compliant Mechanisms, United Kingdom: WILEY, 2013.
- [2] L. Saggere and S. Kota, "Synthesis of Planar, Compliant Four-Bar Mechanisms for Compliant-Segment Motion Generation," *Journal of Mechanical Design*, 2001.
- [3] P. Valentini and E. Pennestri, "Compliant four-bar linkage synthesis with second-order flexure hinge approximation," in *Mechanism and Machine Theory*, 2018.
- [4] L. Zentner, Nachgiebige Mechanismen, Munich: De Gruyter Oldenbourg, 2014.
- [5] E. Hermoza, "Development of methods for the synthesis of compliant mechanisms," Ilmenau, Germany, 2019.
- [6] S. Henning and S. a. Z. L. Linß, "Numerical Calculation of Compliant Four-Bar Mechanisms with Flexure Hinges," *4th International Conference Mechanical Engineering in XXI Century*, 2018.
- [7] J. Vidosic and D. Tesar, "Selection of four-bar mechanisms having required approximate straight-line outputs Part I. The general case of the ball-burmester point," in *Journal of Mechanisms*, 1967.
- [8] L. Cao, A. Dolovich and J. a. Z. W. Herder, "Toward a Unified Design Approach for Both Compliant Mechanisms and Rigid-Body Mechanisms: Module Optimization," *Journal of Mechanical Design*, 2015.
- [9] S. Linß, Ein Beitrag zur geometrischen Gestaltung und Optimierung prismatischer Festkörpergelenke in nachgiebigen Koppelmechanismen, Ilmenau: Universitätsverlag Ilmenau, 2015.
- [10] J. Rodriguez, Resistencia de materiales 2, Lima: Editorial PUCP, 2009.
- [11] B. Deshmukh, S. Pardeshi, S. Mistry, S. Kandharkar and S. Wagh, "Development of a Four bar Compliant Mechanism using Pseudo Rigid Body Model (PRBM)," *3rd International Conference on Materials Processing and Characterisation (ICMPC 2014)*, 2014.
- [12] S. Henning and S. a. Z. L. Linß, "detasFLEX – A computational design tool for the analysis of various notch flexure hinges based on non-linear modeling," *Mechanical Sciences*, 2018.

## CONTACTS

Estefania Hermoza-Llanos

email: [hermoza-llanos@igmr.rwth-aachen.de](mailto:hermoza-llanos@igmr.rwth-aachen.de)

ORCID: <https://orcid.org/0000-0003-2764-4861>

Prof. Dr. Ing. Jorge Rodríguez Hernández  
Univ.-Prof. Dr.-Ing. habil. Lena Zentner

email: [crodrig@pucp.edu.pe](mailto:crodrig@pucp.edu.pe)

email: [lena.zentner@tu-ilmenau.de](mailto:lena.zentner@tu-ilmenau.de)

ORCID: <https://orcid.org/0000-0003-4219-9006>